SAND2022-9029C

Sandia National Laboratories

Recovery of forsterite high-pressure polymorphs in gas gun shock-wave experiments

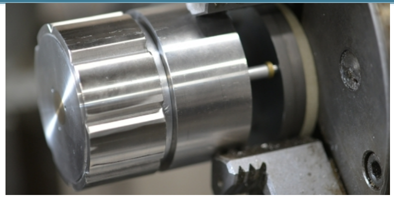

Mans, W. M., Knudson, M., Cochran, K., & Townsend, J. P.

22nd Biennial Conference of the American Physical Society Topical Group on Shock Compression of Condensed Matter 2022 – July 13

U.S. DEPARTMENT OF ENERGY NNSA

Sandia National Laboratories is a multimission laboratory managed and operated by National Technology & Engineering Solutions of Sandia, LLC, a wholly owned subsidiary of Honeywell International Inc., for the U.S. Department of Energy's National Nuclear Security Administration under contract DE-NA0003525.

Outline

- 1. Background:
  Study of high-pressure phases of olivine in meteorites
- 2. Methods:
  Experimental details and process
- 3. Results:
  From initial shock experiment campaign
- 4. Path forward

Outline

- 1. Background:
  Study of high-pressure phases of olivine in meteorites
- 2. Methods:
  Experimental details and process
- 3. Results:
  From initial shock experiment campaign
- 4. Path forward

Ultrafast growth of wadsleyite in shock-produced melts and its implications for early solar system impact processes

Oliver Tschauner, Paul D. Asimow,
Natalya Kostandova, Thomas J. Ahrens,
Chi Ma, Stanislas Sinogeikin, Zhenxian Liu,
Sirine Fakra, and Nobumichi Tamura

nature COMMUNICATIONS

Ultrafast olivine-ringwoodite transformation during shock compression

Takuo Okuchi, Yusuke Seto, Naotaka Tomioka, Takeshi Matsuoka, Bruno Albertazzi, Nicholas J. Hartley, Yuichi Inubushi, Kento Katagiri, Ryosuke Kodama, Tatiana A. Pikuz, Narangoo Purevjav, Kohei Miyanishi, Tomoko Sato, Toshimori Sekine, Keiichi Sueda, Kazuo A. Tanaka, Yoshinori Tange, Tadashi Togashi, Yuhei Umeda, Toshinori Yabuuchi, Makina Yabashi & Norimasa Ozaki

Table 2. High-pressure minerals in chondrites. (Tomioka & Miyahara, 2017)

Meteorites	Type	Wds	Rwd	Ahr	Jad	Maj	Maj-Prp	Aki	Hem	Bdg	Lin	Coe	Sti	Tui	Refs.
GRV 052049	L5		X												1
Yamato-8410	L5				X										2
Roy	L5/6		X			X									3
Taiban	L5	X	X		X	X	X				X				4
Acfer 040	L5/6		X					X		X[a]					5, 6
Chelyabinsk	LL5				X										7
Novosibirsk	H5/6				X										8
Yamato-75100	H6	X	X		X	X	X	X			X				2, 9–11
Yamato-75267	H6	X	X		X	X	X	X			X				12
Allan Hills 78003	L6	X	X		X	X	X								13, 14
Asuka-09584	L6	X	X												15
Catherwood	L6		X			X									16
Coolamon	L6		X												17
Coorara	L6		X			X									17, 18
Dhofar 922	L6		X												19
GRV 022321	L6		X												20
GRV 052082	L6		X		X	X	X	X			X				21–22
Mbale	L5/6	X	X				X								5, 22, 23
NWA 5011	L6		X			X	X								24, 25
Peace River	L6	X	X		X		X	X							26–28
Sahara 98222	L6	X			X										29
Sixiangkou	L6	X	X		X	X	X	X			X				30–35
Suizhou	L6		X			X	X	X	X	X[a]	X			X	36–40
Tenham	L6	X	X			X	X	X		X	X				41–47
Umbarger	L6		X	X				X			X		X		3, 48, 49
Yamato-74445	L6	X	X		X	X	X	X			X			X	14, 29
Yamato-790729	L6		X			X		X			X				50
Yamato-791384	L6		X		X	X	X	X			X				9, 13, 51, 52
Roosevelt County 106	L6		X		X	X					X				53
Sahara 00293	L6	X	X												54
Pervomaisky	L6				X		X								55
NWA 757	LL6	X	X								X			X	56, 57
Asuka-10164	EH3											X			58
Gujba	CB	X	X		X	X		X			X	X			59, 60
Khatyrka	CV3			X								X	X		61, 62

[a]Described as vitrified bridgmanite.

[1]Feng et al. (2011), [2]Kimura et al. (2001), [3]Xie et al. (2006a), [4]Acosta-Maeda et al. (2013), [5]Sharp and Hu (2016), [6]Sharp et al. (1997), [7]Ozawa et al. (2014), [8]Bazhan et al. (2017a), [9]Miyahara et al. (2013b), [10]Miyahara et al. unpublished data, [11]Tomioka and Kimura (2003), [12]Kimura et al. (2003), [13]Ohtani et al. (2006), [14]Miyahara et al. (2009), [15]Pittarello et al. (2015), [16]Coleman (1977), [17]Steele and Smith (1978), [18]Smith and Mason (1970), [19]Badjukov et al. (2005), [20]Xie et al. (2010), [21]Feng et al. (2017), [22]Chen et al. (1998), [23]Sharp et al. (1996), [24]Nagy et al. (2010), [25]Nagy et al. (2011), [26]Chen et al. (1996a), [27]Miyahara et al. (2008), [28]Price et al. (1983), [29]Ozawa et al. (2009), [30]Chen et al. (1996b), [31]Chen et al. (2004), [32]Chen et al. (2007), [33]Chen and Xie (2008), [34]Gillet et al. (2000), [35]Zhang et al. (2006), [36]Chen and Xie (2015), [37]Xie et al. (2001), [38]Xie et al. (2002a), [39]Xie et al. (2011a), [40]Bindi et al. (2017), [41]Langenhorst et al. (1995), [42]Putnis and Price (1979), [43]Tomioka and Fujino (1997), [44]Tomioka et al. (2000), [45]Tschauner et al. (2014), [46]Xie et al. (2006b), [47]Xie and Sharp (2007), [48]Xie and Sharp (2004), [49]Xie et al. (2002b), [50]Kato et al. (2012), [51]Miyahara et al. (2010), [52]Ohtani et al. (2004), [53]Sharp et al. (2015), [54]Fudge et al. (2014), [55]Bazhan et al. (2017b), [56]Bischoff (2002), [57]Hu and Sharp (2016), [58]Kimura et al. (2017), [59]Weisberg and Kimura (2010), [60]Miyahara et al. (2015), [61]Bindi et al. (2014), [62]Hollister et al. (2014).

Wds = wadsleyite, Rwd = ringwoodite, Ahr = ahrensite, Jad = jadeite, Maj = majorite, Maj-Prp = majorite-pyrope solid solution, Aki = akimotoite, Hem = hemleyite, Bdg = bridgmanite, Lin = liuguite, Coe = coesite, Sti = stishovite, Tui = tuite.

Ordinary Chondrites

Wadsleyite

Ringwoodite

Table 3. High-pressure minerals in achondrites and iron meteorite.

Meteorites	Type	Wds	Rwd	Ahr	Tis	Maj	Aki	Bdg	Lin	Lie	Coe	Sti	Sei	CAS	Tui	Xie	Refs.
Asuka-881757	Lunar (gabbro)										X	X					1
NWA 4734	Lunar (basalt)										X	X	X				2
NWA 479	Lunar (basalt)	X	X														3
NWA 2977	Lunar (gabbro)		X														4
NWA 2727	Lunar (basalt/gabbro breccia)										X	X					5
Apollo 15299	Lunar (regolith breccia)											X					6
DaG 735	Maritian (shergottite)							X[a]									7
DaG 670	Maritian (shergottite)		X														8
Tissint	Maritian (shergottite)		X	X	X	X	X	X[a]	X			X			X		9–12
EETA 79001	Maritian (shergottite)		X														13
Zagami	Maritian (shergottite)						X	X[a]	X	X		X	X	X			14–18
NWA 480	Maritian (shergottite)											X		X			14, 15
NWA 856	Maritian (shergottite)								X			X	X	X			14, 15
NWA 1068	Maritian (shergottite)											X		X			14
NWA 4468	Maritian (shergottite)		X									X			X		19
Los Angeles	Maritian (shergottite)													X			14
SaU 005	Maritian (shergottite)											X		X			14
Shergotty	Maritian (shergottite)					X			X			X	X	X			14, 20, 21
NWA 2975	Maritian (shergottite)											X					22
GRV 020090	Maritian (shergottite)		X			X	X								X		23, 24
Yamato-000047	Maritian (shergottite)						X										25
Chassigny	Martian (chassignite)	X	X					X[a]							X	X	20, 26
Béréba	Eucrite (monomict breccia)										X	X					27
NWA 8003	Eucrite				X						X	X					28
Muonionalusta	Iron (IVA)											X					29

[a]Described as vitrified bridgmanite.

[1]Ohtani et al. (2011), [2]Miyahara et al. (2013a), [3]Barrat et al. (2005), [4]Zhang et al. (2010), [5]Kayama et al. (2016), [6]Kaneko et al. (2015), [7]Miyahara et al. (2011), [8]Greshake et al. (2013), [9]Baziotis et al. (2013), [10]Ma et al. (2015), [11]Miyahara et al. (2016), [12]Walton et al. (2014), [13]Walton-Hauck (2012), [14]Beck et al. (2004), [15]El Goresy et al. (2013), [16]Langenhorst and Poirier (2000a), [17]Langenhorst and Poirier (2000b), [18]Ma et al. (2014), [19]Boonsue and Spray (2012), [20]Malavergne et al. (2001), [21]Sharp et al. (1999), [22]He et al. (2015), [23]Lin et al. (2011), [24]Lin et al. (2012), [25]Imae and Ikeda (2010), [26]Fritz and Greshake (2009), [27]Miyahara et al. (2014), [28]Pang et al. (2016), [29]Holtstam et al. (2003).

Wds = wadsleyite, Rwd = ringwoodite, Ahr = ahrensite, Tis = tissintite, Maj = majorite, Aki = akimotoite, Bdg = bridgmanite, Lin = lingunite, Lie = liebermannite, Coe = coesite, Sti = stishovite, Sei = seifertite, CAS = Ca-Al-Si-rich phase, Tui = tuite, Xie = xieite.

(Tomioka & Miyahara, 2017)

Lunar & Martian

Wadsleyite

Ringwoodite

Initial shot-campaign goals

- 1. Refinement of recovery assembly to preserve samples through a higher velocity/pressure range
- 2. Shock recovery of high-pressure olivine phases
- 3. Detailed examination of shock effects and features over a range of pressures
- 4. Developing hydrocode models that represent the dynamic shock systems
- 5. Exploration of conductive materials and minerals on high-pressure phase preservation

Outline

- 1. Background:
  Study of high-pressure phases of olivine in meteorites
- 2. Methods:
  Experimental details and process
- 3. Results:
  From initial shock experiment campaign
- 4. Path forward

GUN CONFIGURATION

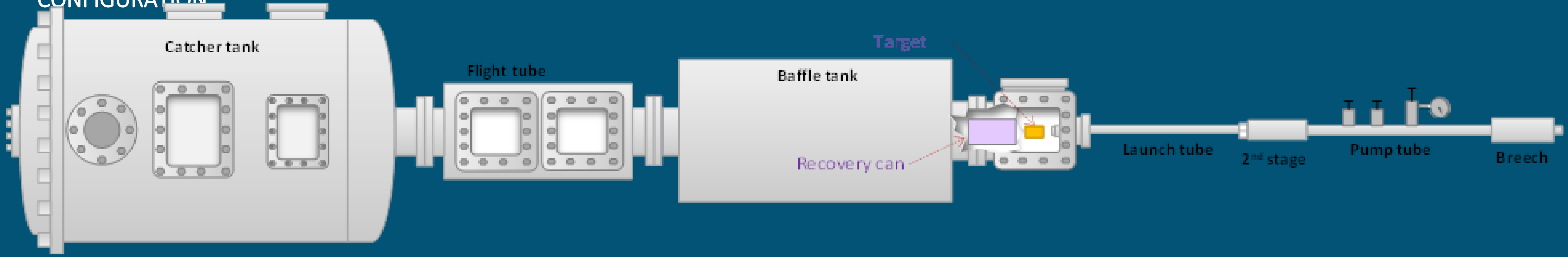

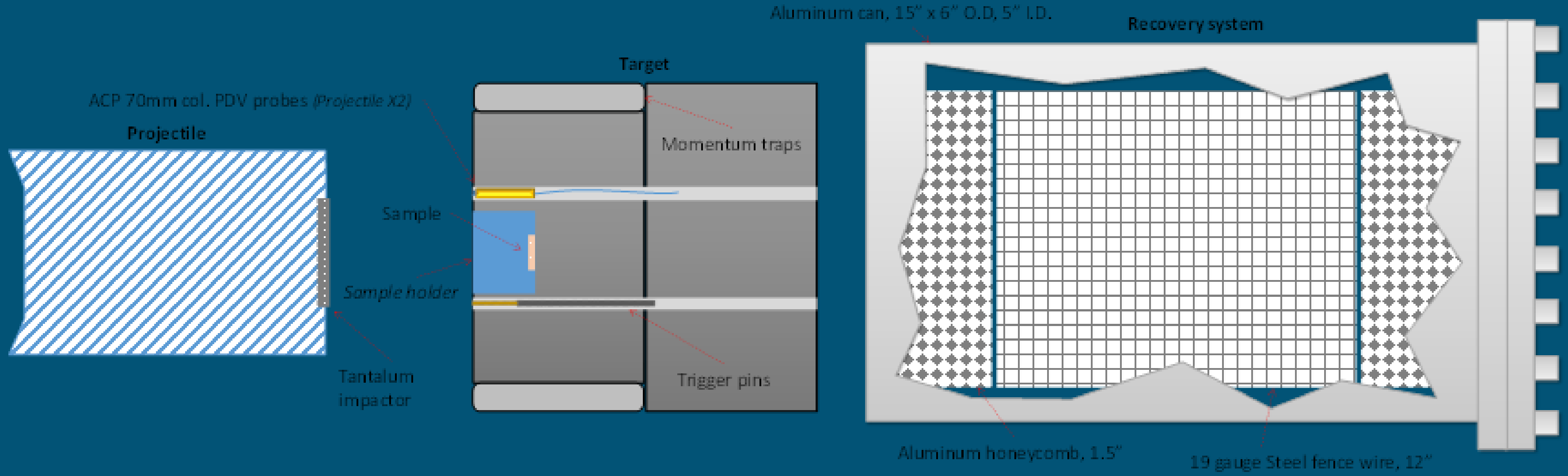

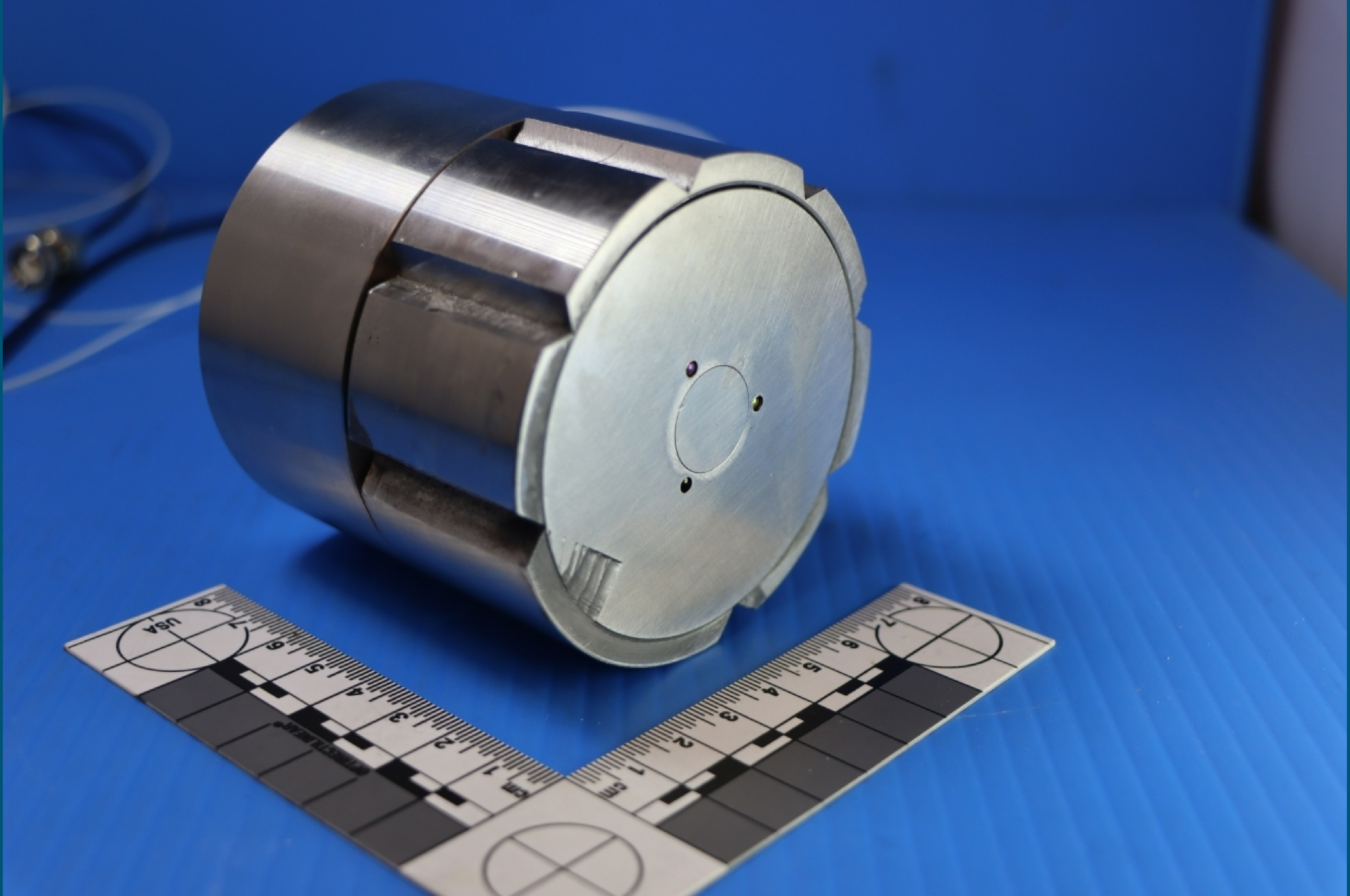

Sample parameters

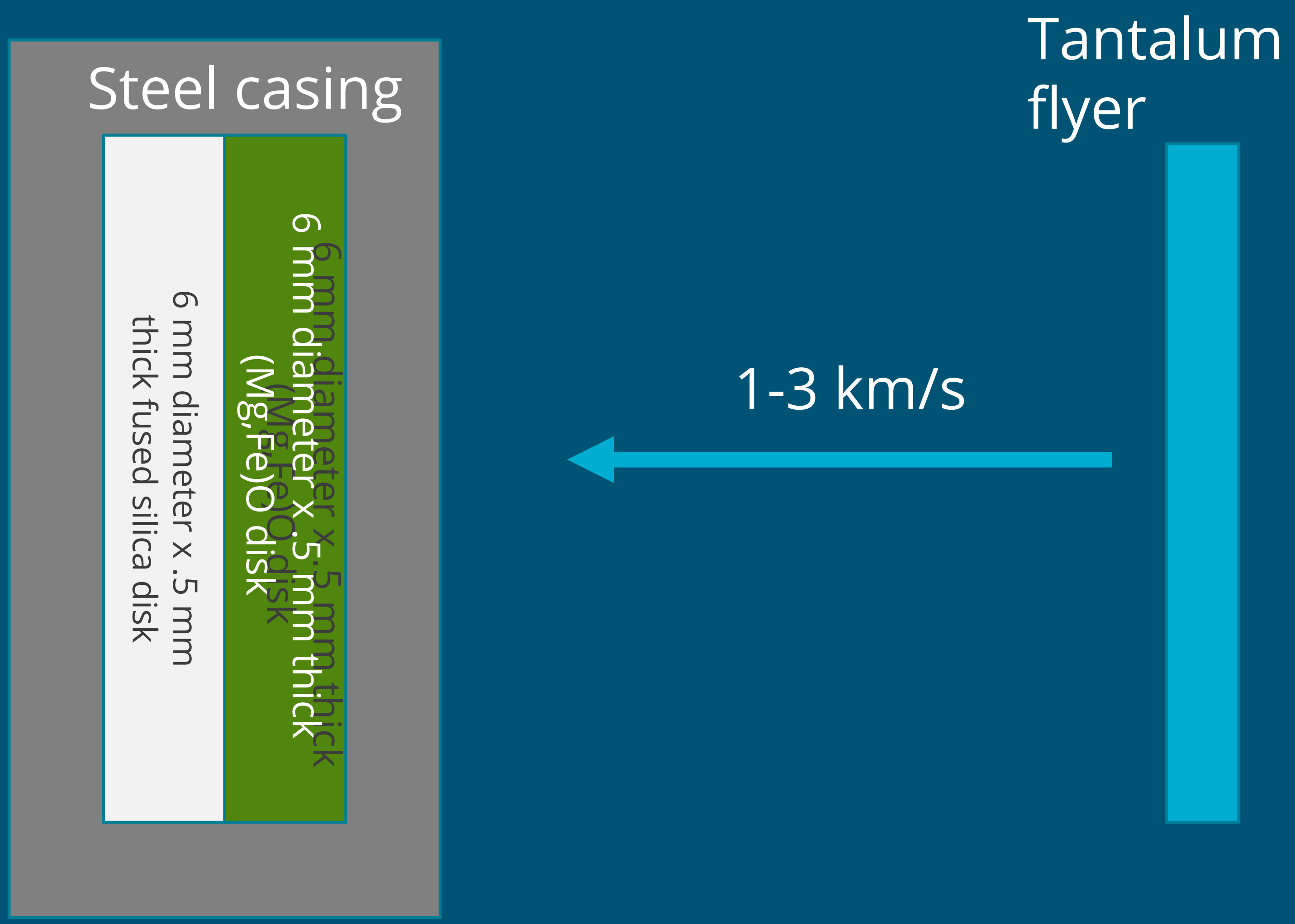

Pressure range (15-40 GPa)

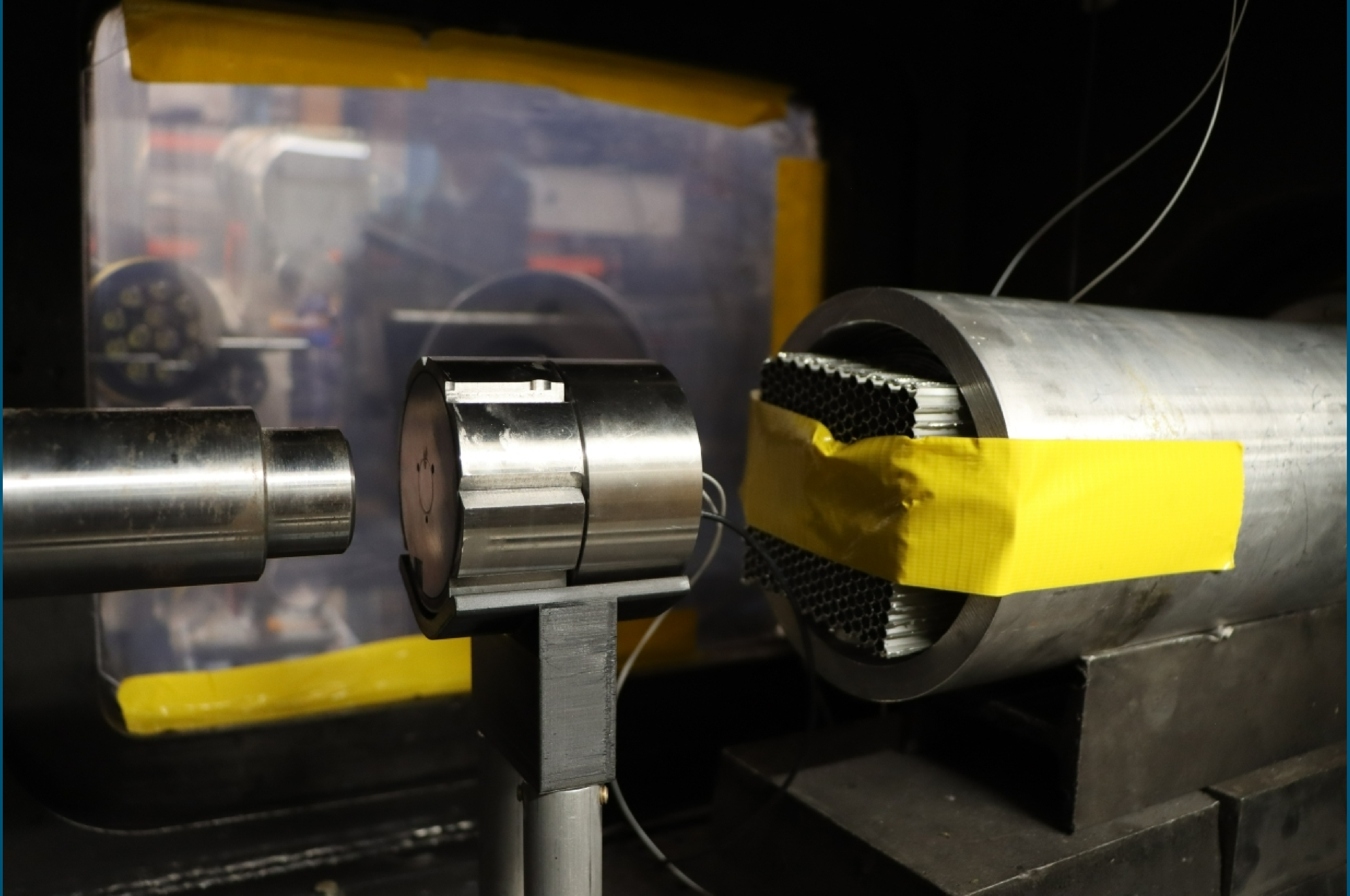

Impact velocity

2.469 km/s

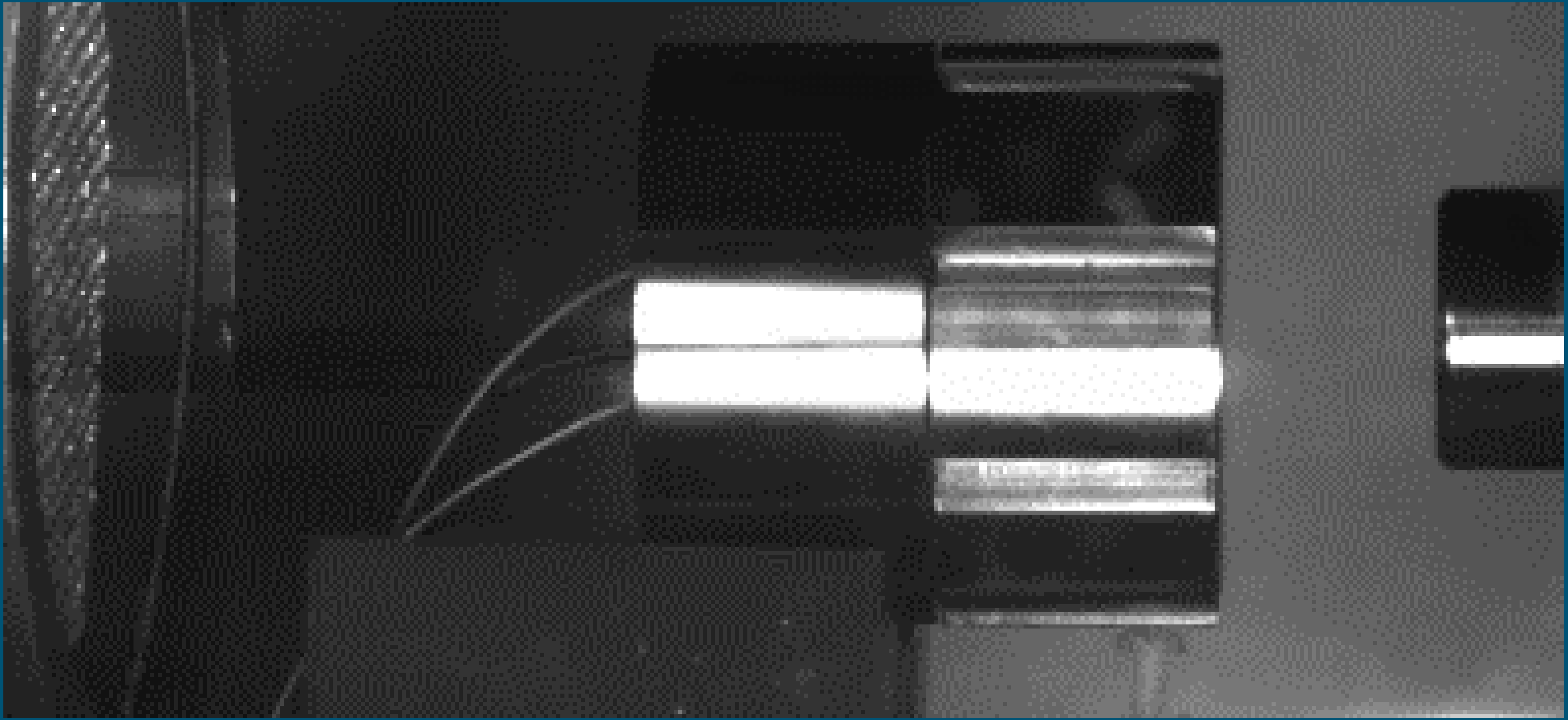

Impact velocity
2.469 km/s

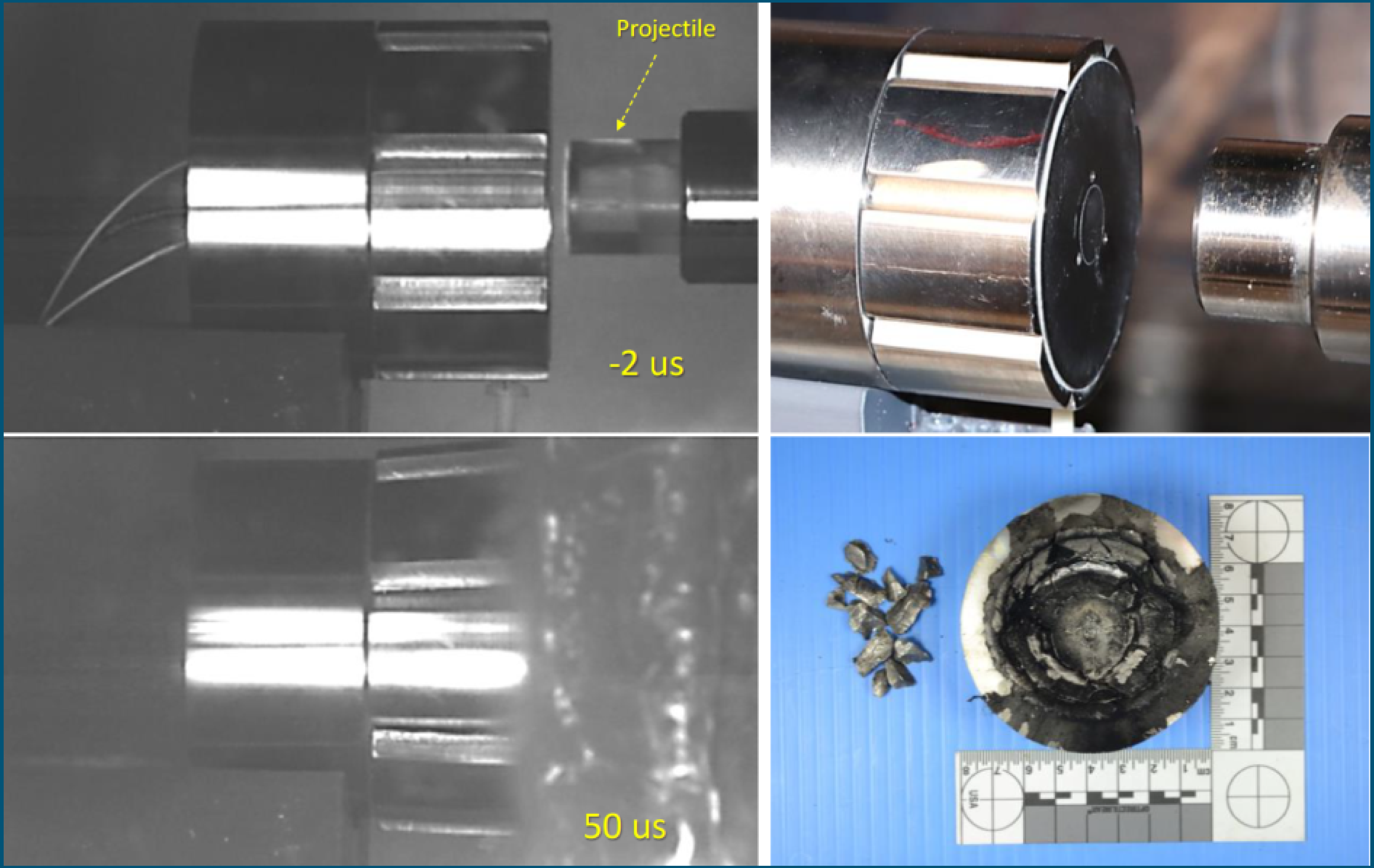

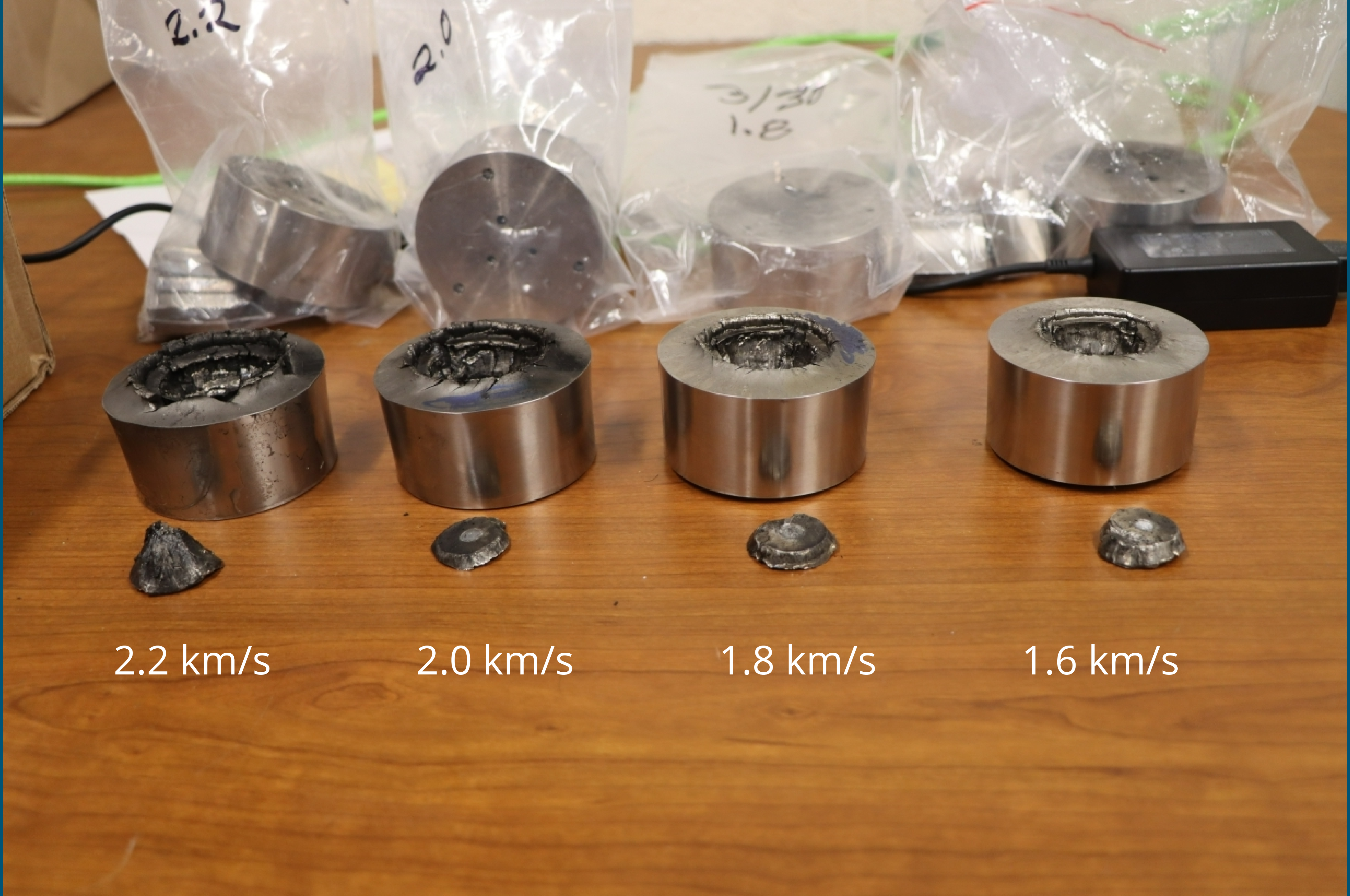
2.2
2.0
3/30
1.8
2.2 km/s
2.0 km/s
1.8 km/s
1.6 km/s

Outline

- 1. Background:
  Study of high-pressure phases of olivine in meteorites
- 2. Methods:
  Experimental details and process
- 3. Results:
  From initial shock experiment campaign
- 4. Path forward

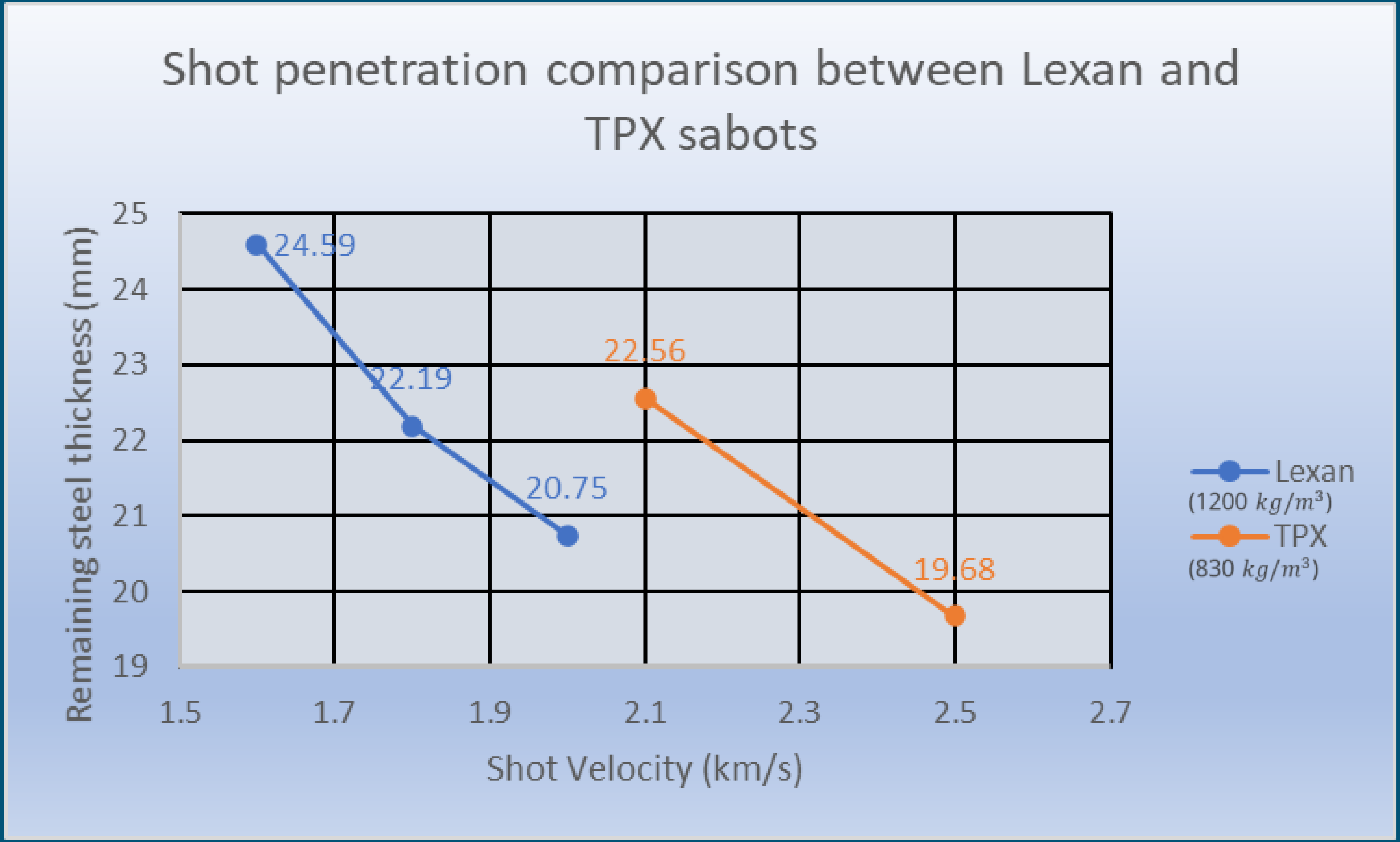
Shot penetration comparison between Lexan and TPX sabots
Remaining steel thickness (mm)
25
24
23
22
21
20
19
1.5
1.7
1.9
2.1
2.3
2.5
2.7
Shot Velocity (km/s)
24.59
22.19
20.75
22.56
19.68
Lexan
(1200 kg/m^3)
TPX
(830 kg/m^3)

Electron microprobe wavelength-dispersive x-ray mapping of 2.2 km/s calibration shot

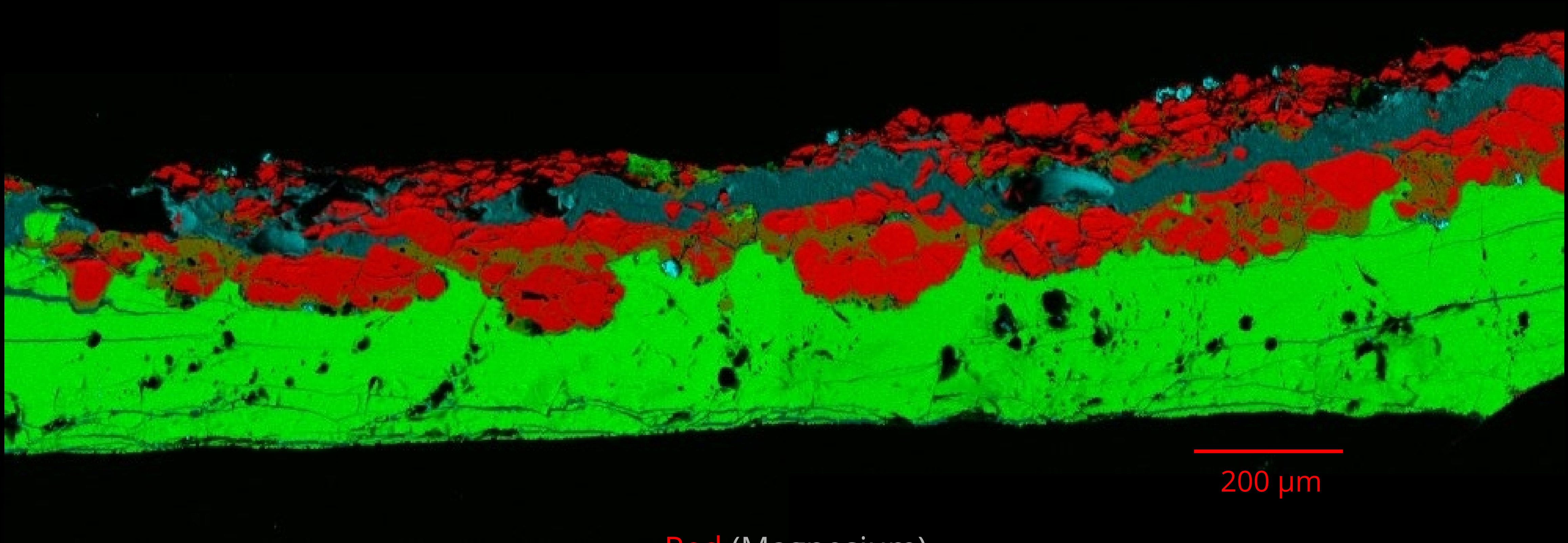

Red (Magnesium)
Cyan (Carbon)
Green (Silica)

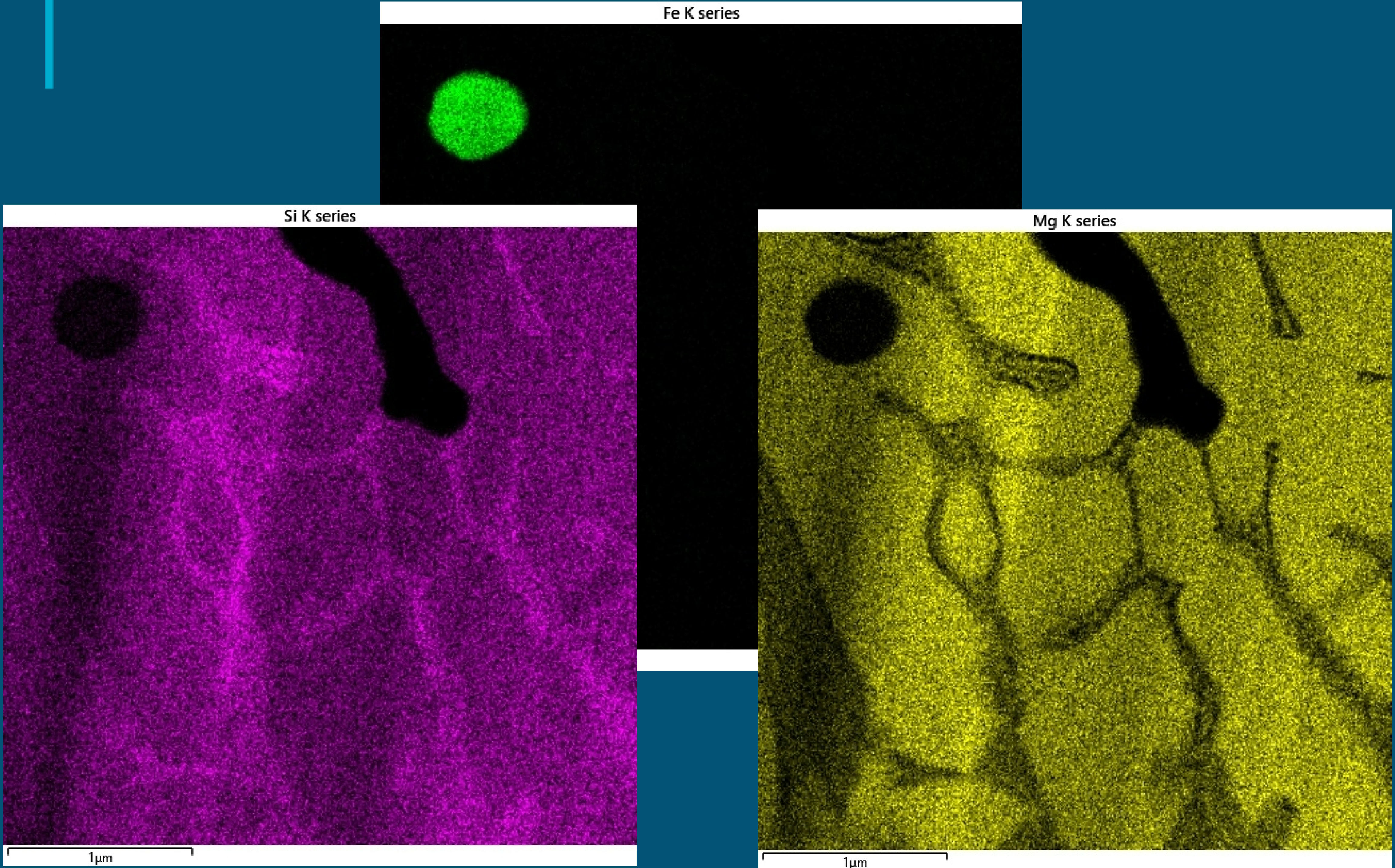
Fe K series
Si K series
1µm
Mg K series
1µm

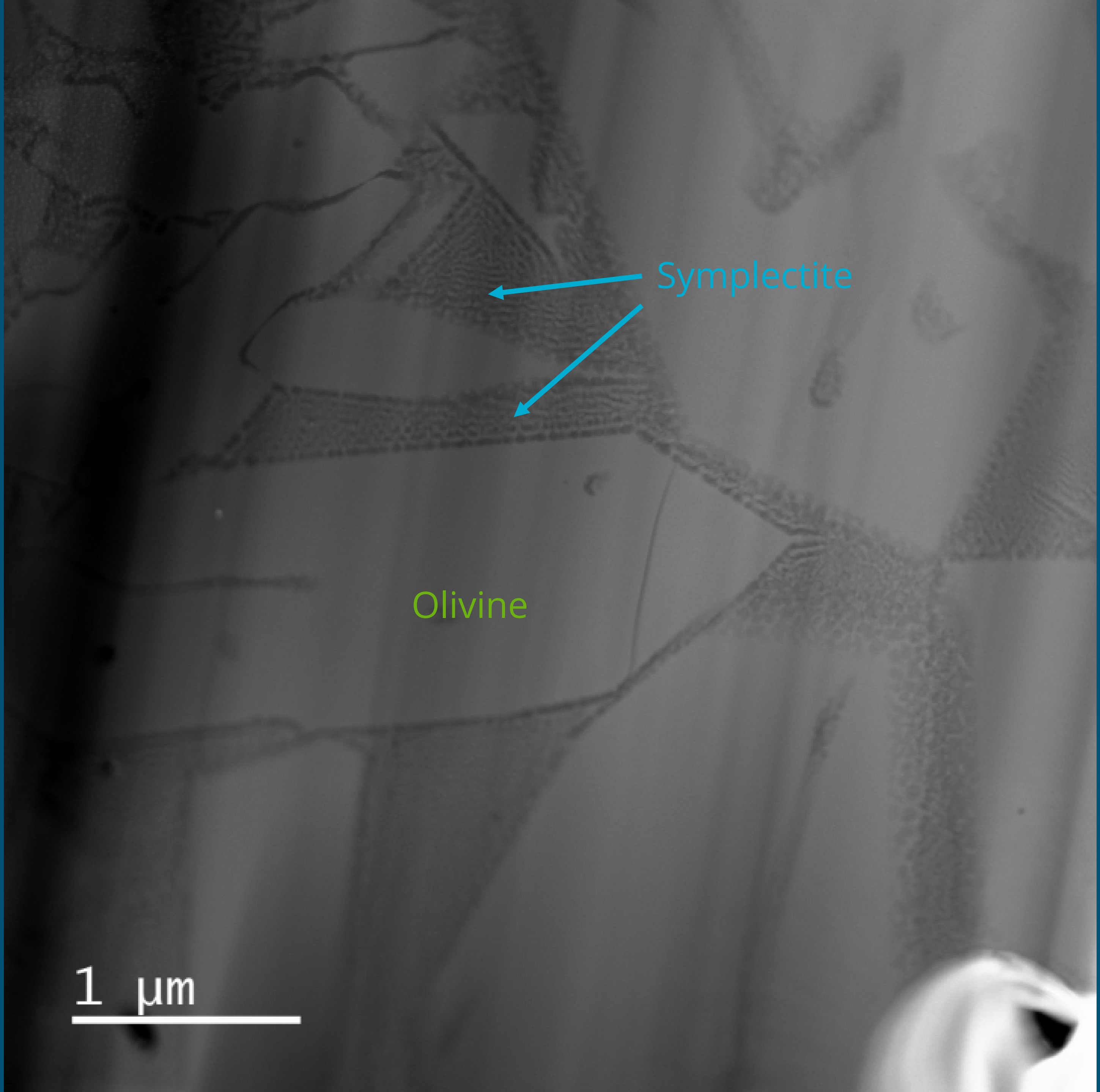
Symplectite
Olivine
1 µm

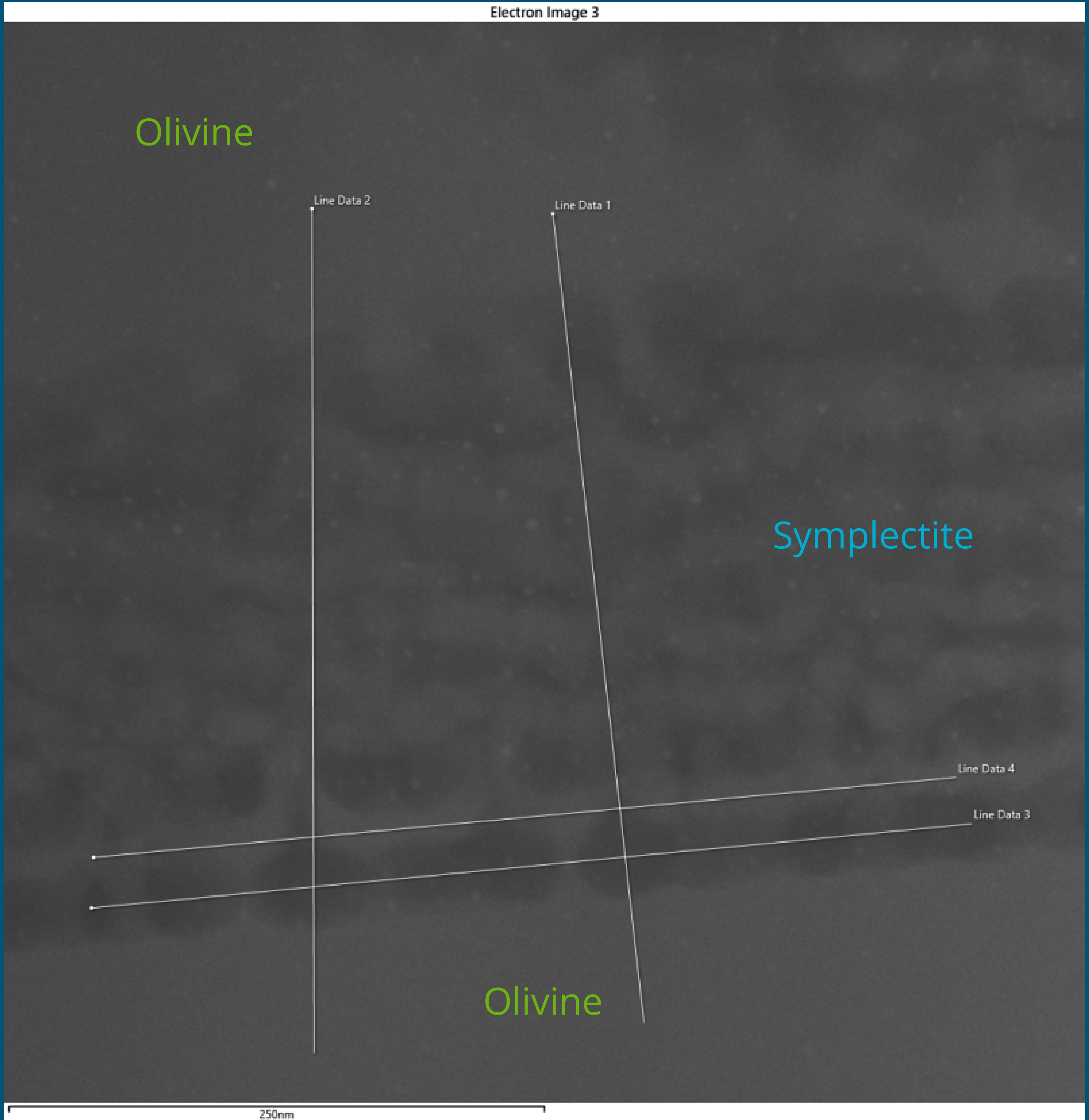
Electron Image 3
Olivine
Line Data 2
Line Data 1
Symplectite
Line Data 4
Line Data 3
Olivine
250nm

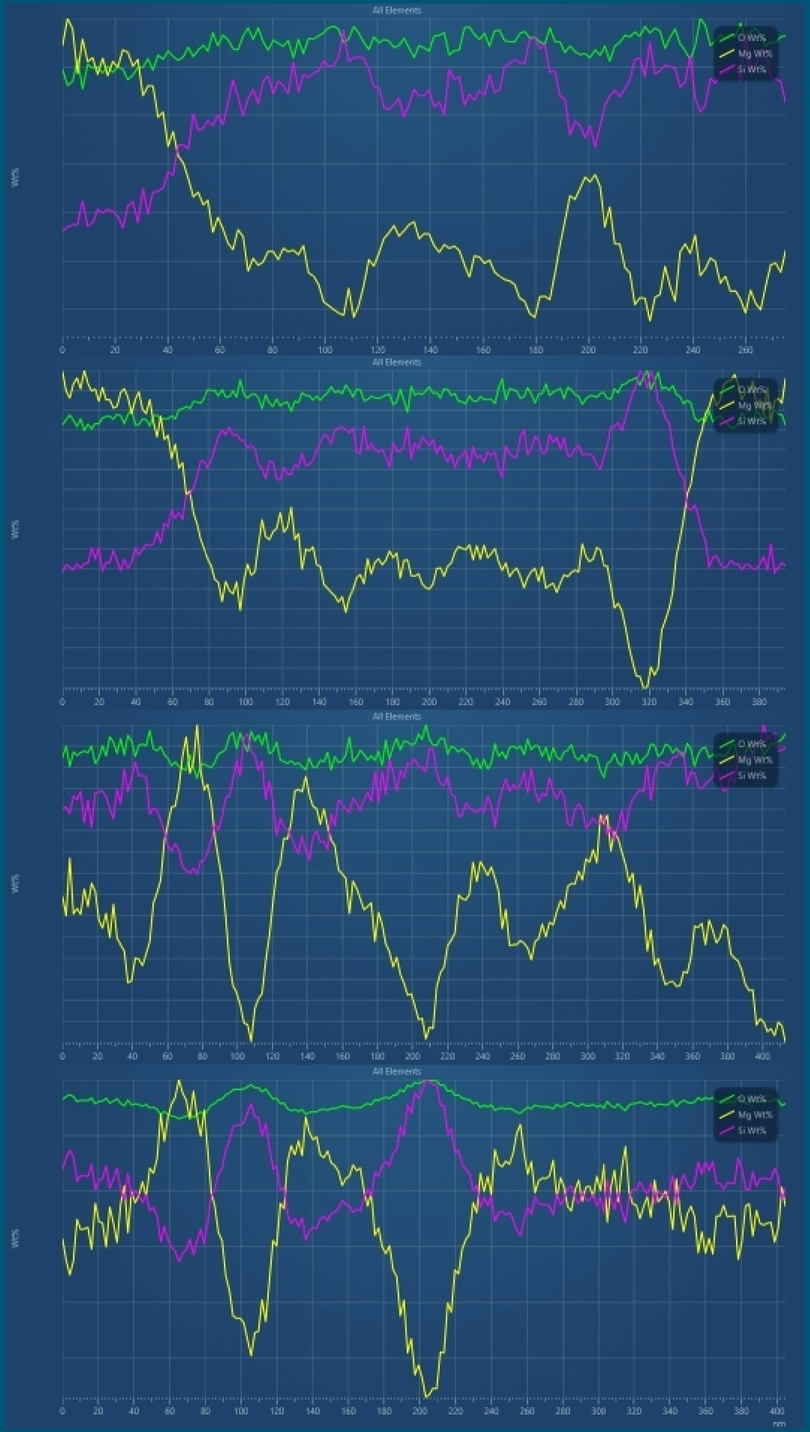
All Elements
O Wt%
Mg Wt%
Si Wt%

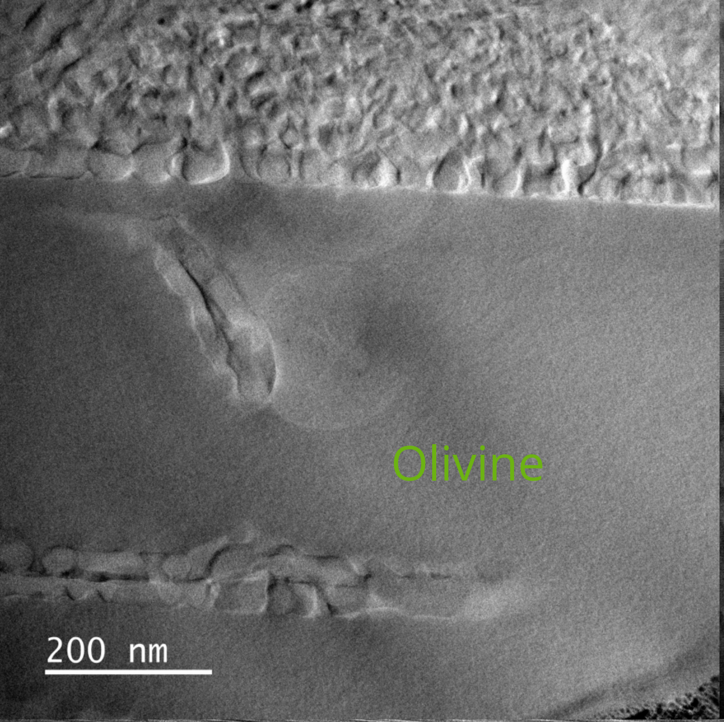
Olivine
200 nm

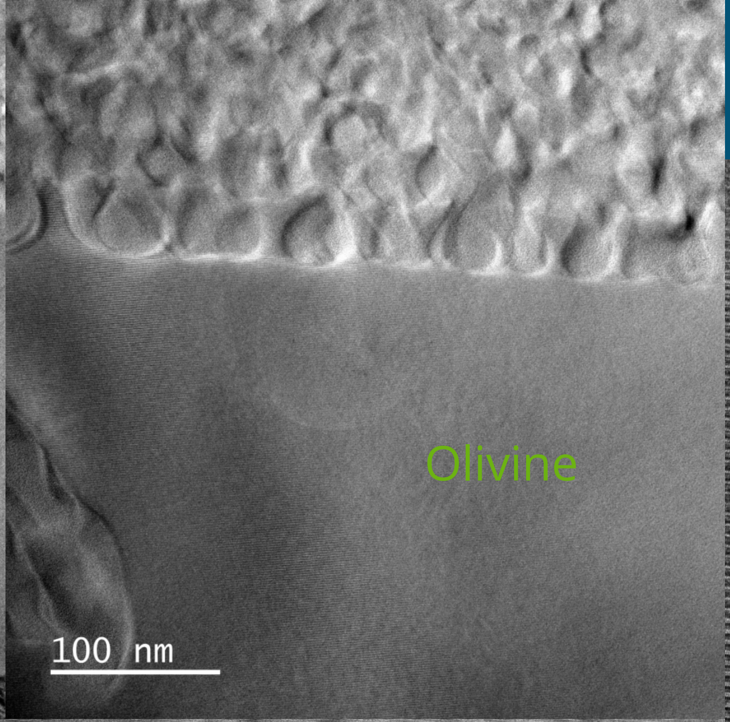
Olivine
100 nm

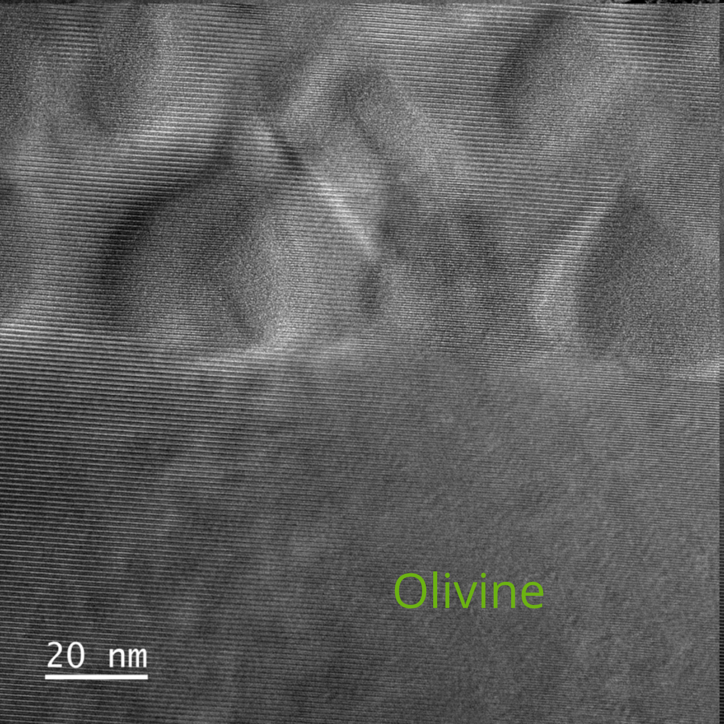
Olivine
20 nm

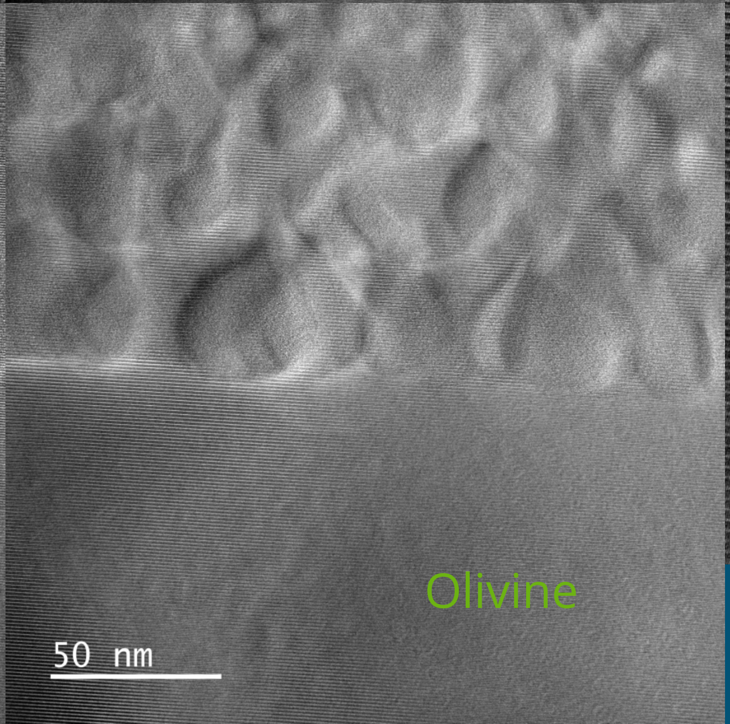
Olivine
50 nm

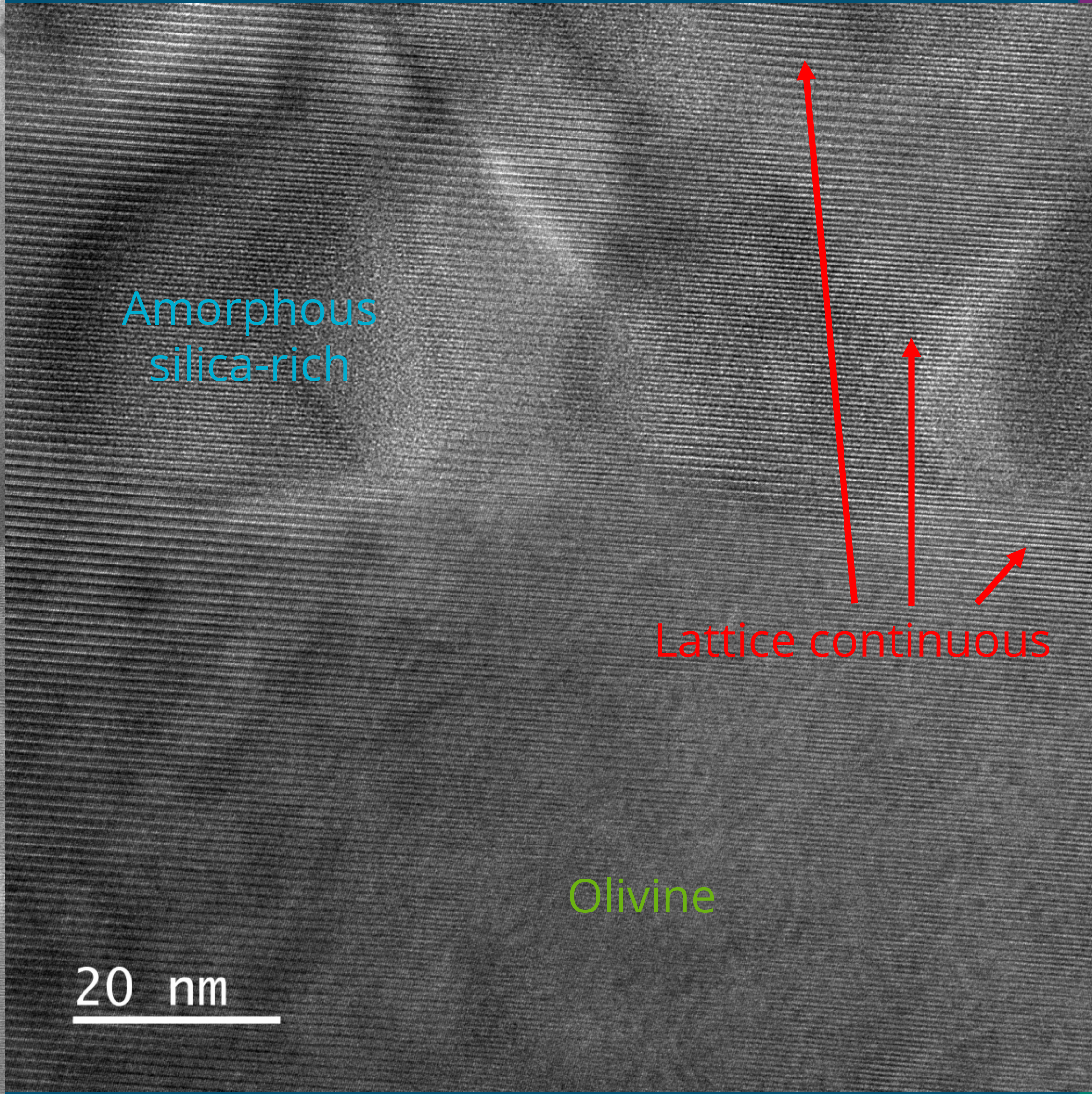
Amorphous
silica-rich
Lattice continuous
Olivine
20 nm

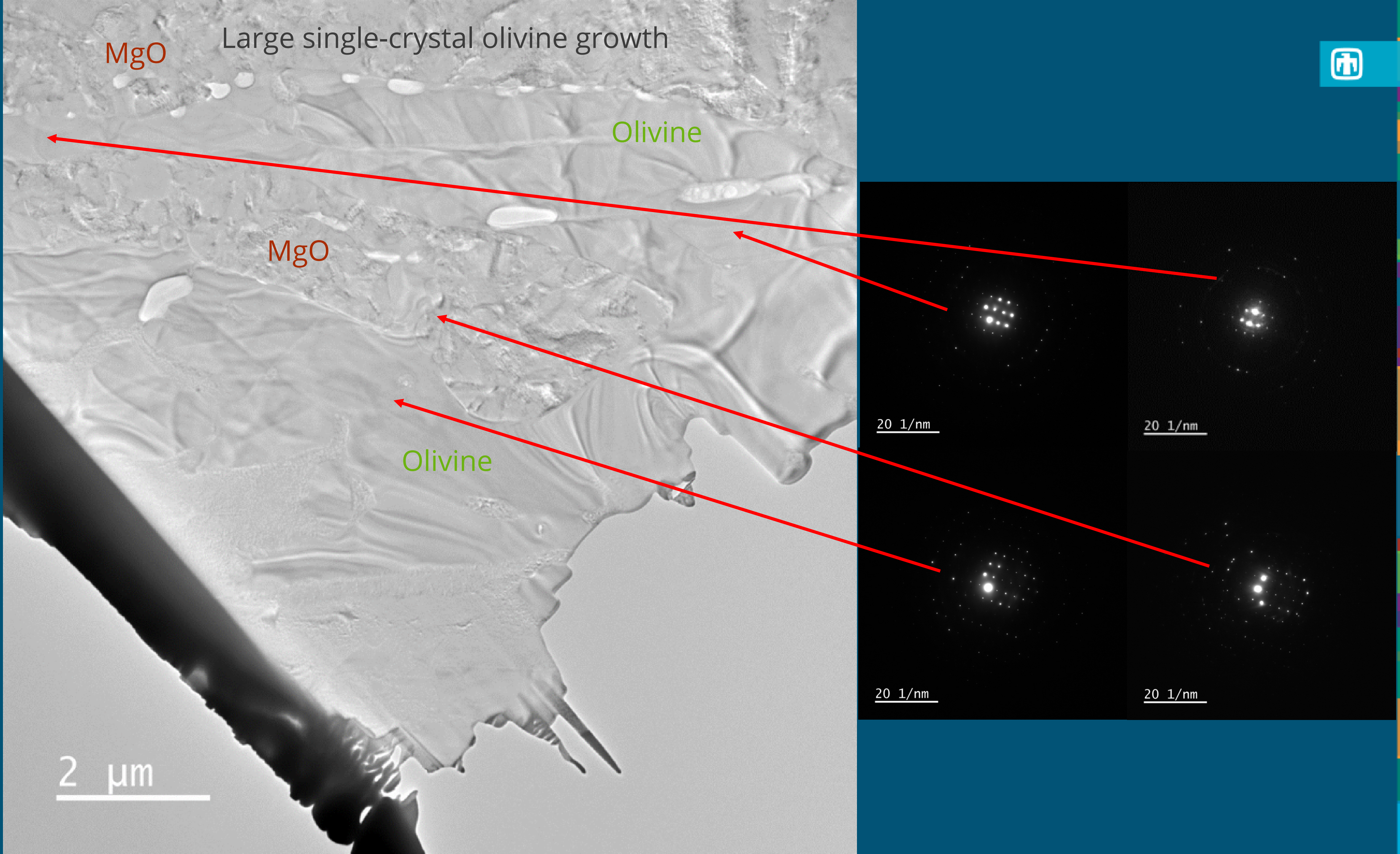

Large single-crystal olivine growth
MgO
Olivine
MgO
Olivine
2 µm
20 1/nm
20 1/nm
20 1/nm
20 1/nm

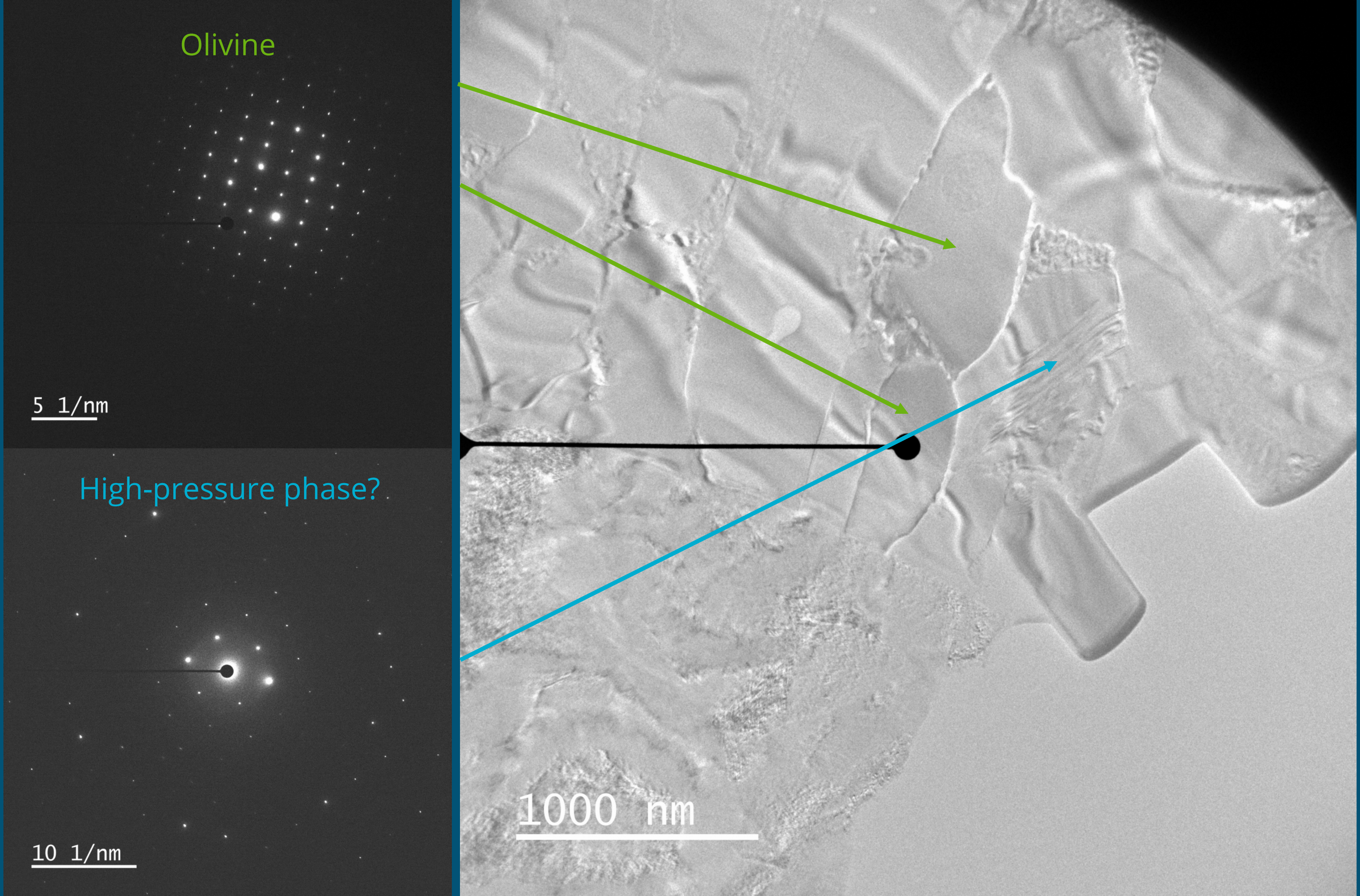
Olivine
5 1/nm
High-pressure phase?
10 1/nm
1000 nm

2.2 km/s lexan sabot shot

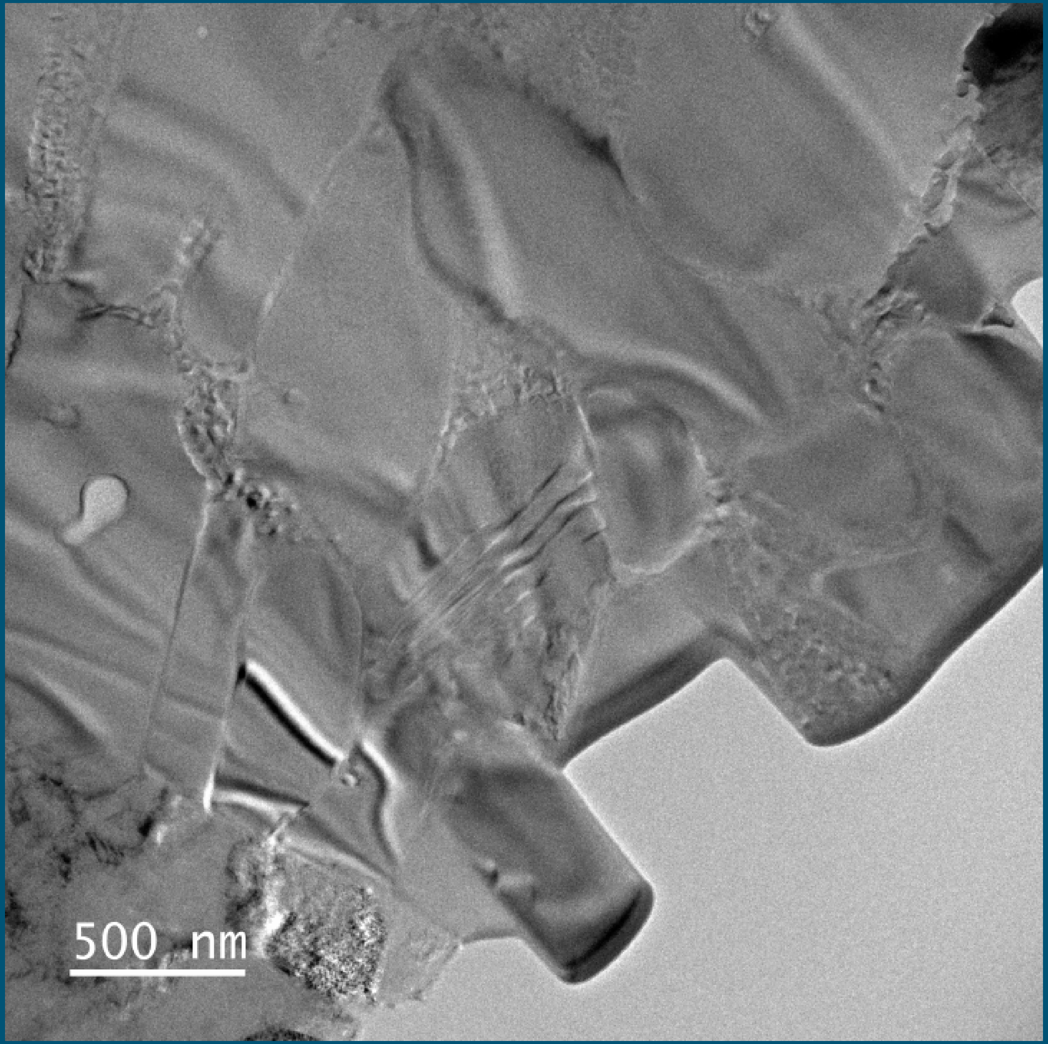

L5-6 Acfer 040 chondrite (Sharp et al., 1997)

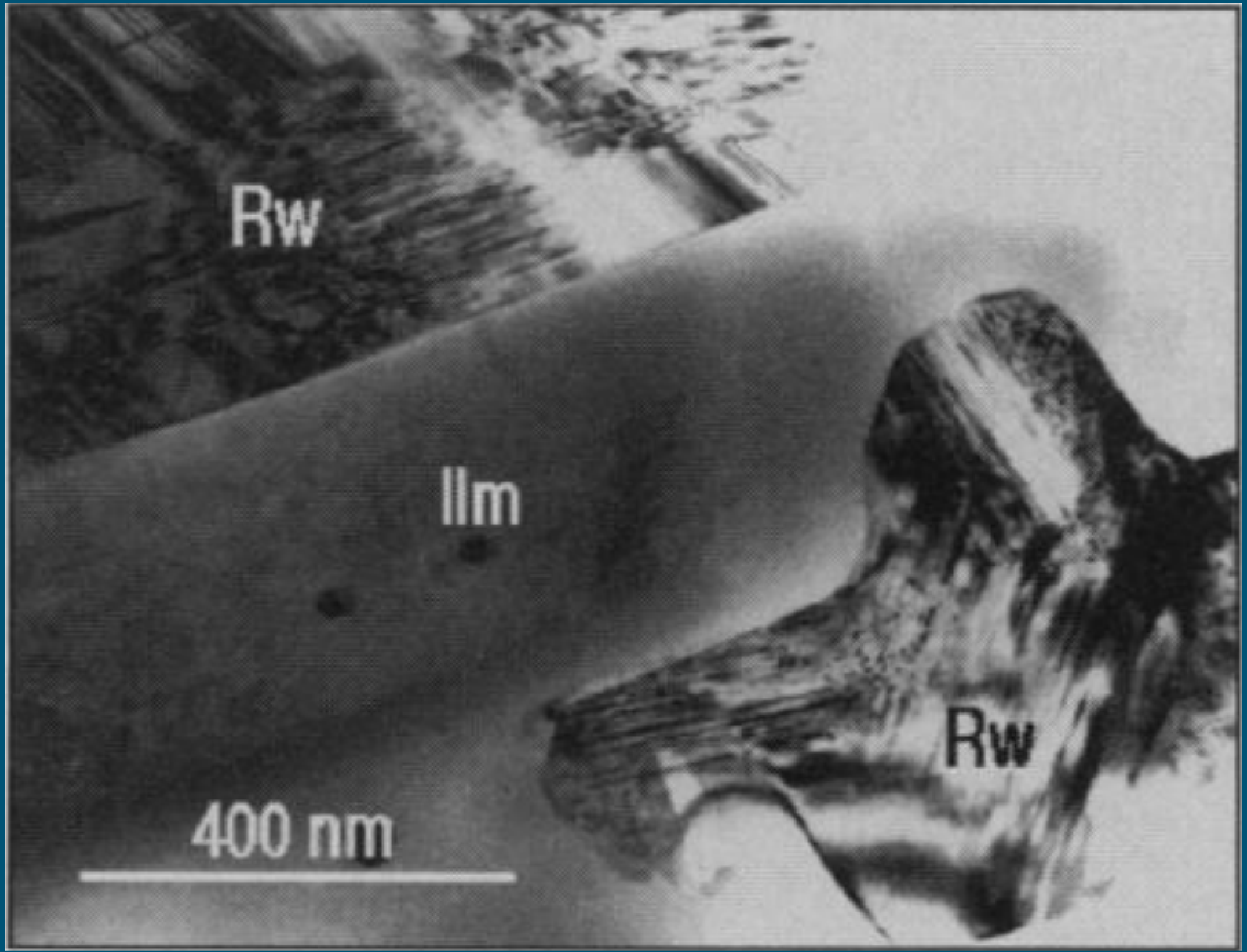

1.6 km/s Core-side

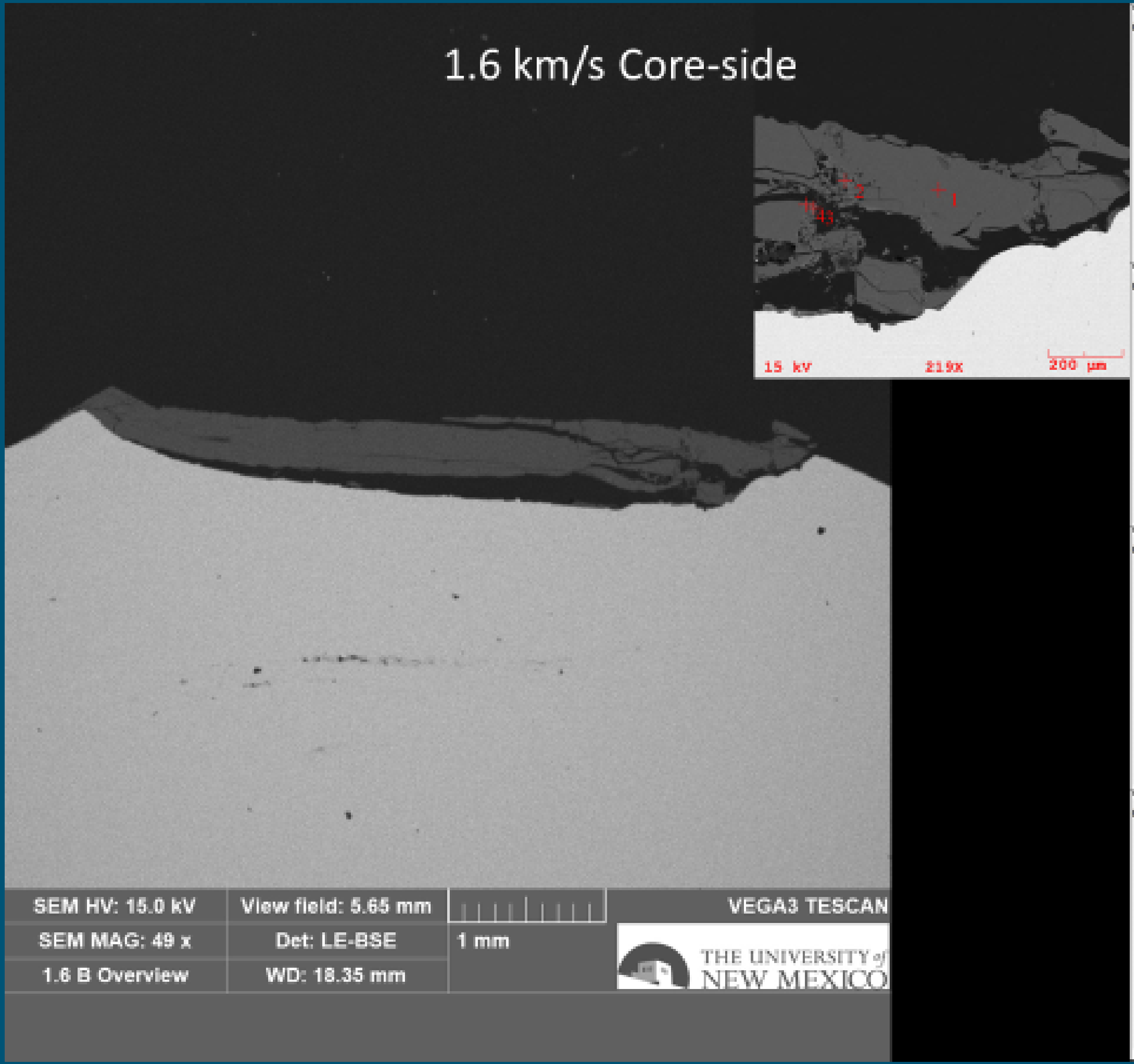

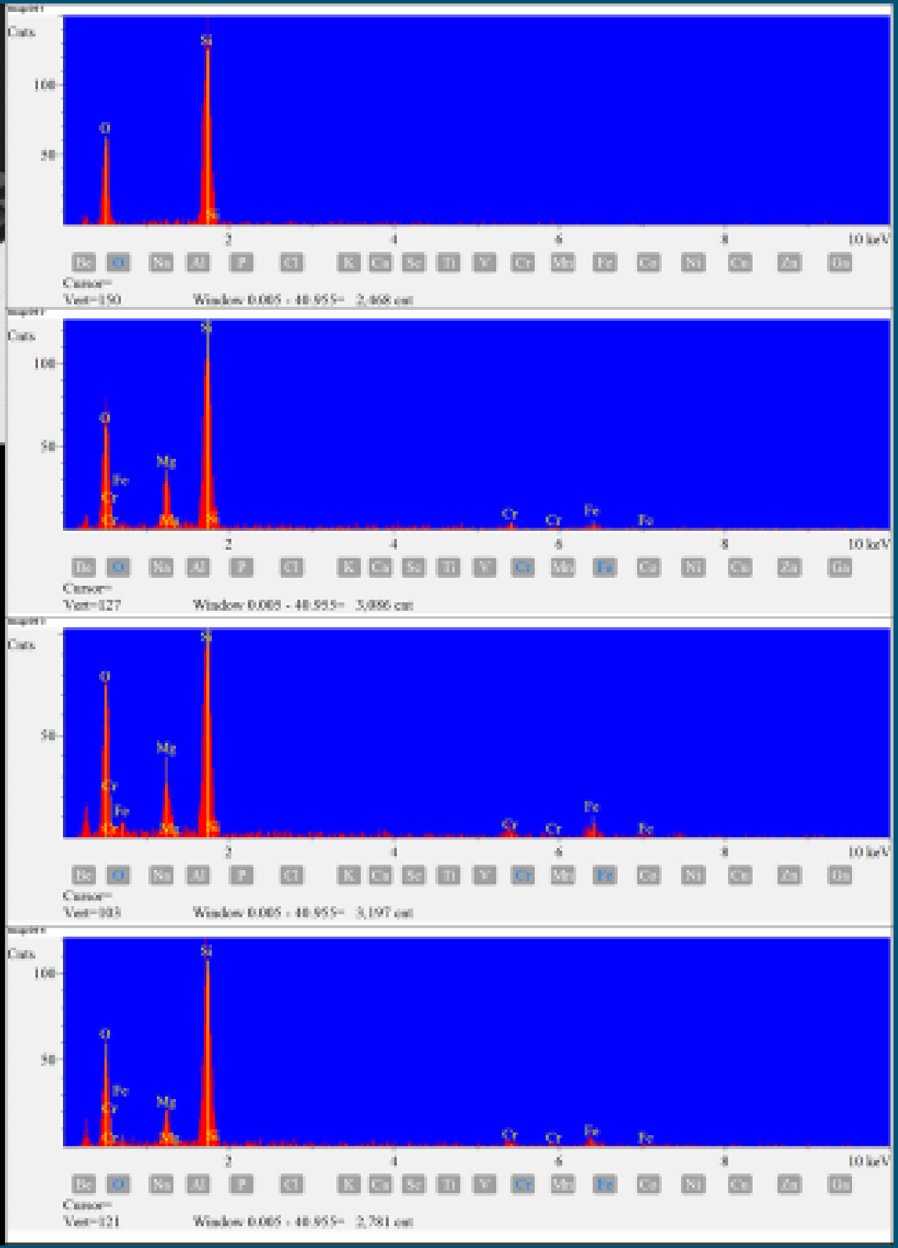

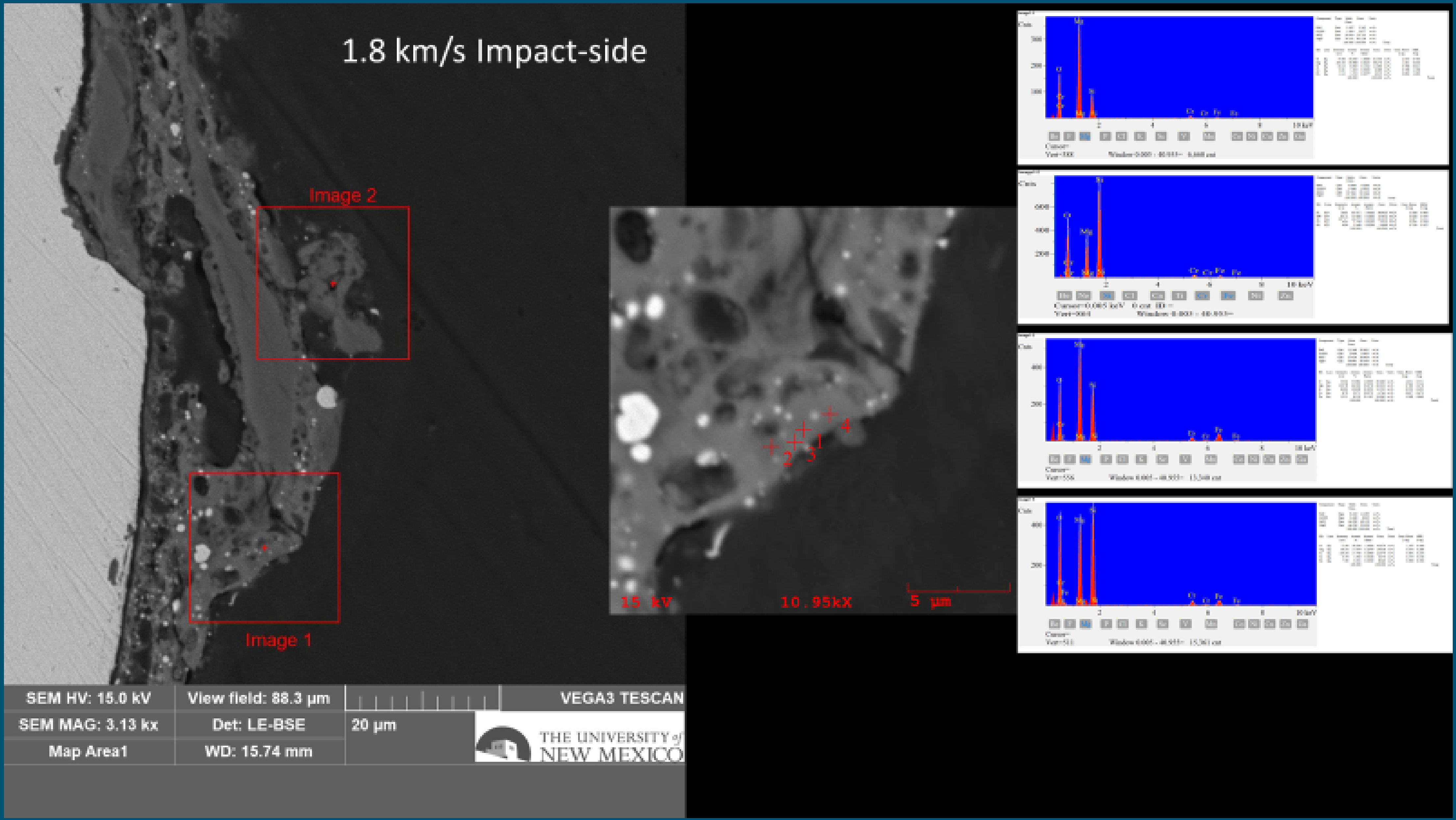
1.8 km/s Impact-side
Image 2
Image 1
SEM HV: 15.0 kV
View field: 88.3 μm
VEGA3 TESCAN
SEM MAG: 3.13 kx
Det: LE-BSE
20 μm
Map Area1
WD: 15.74 mm
THE UNIVERSITY of NEW MEXICO
1
2
3
4
15 kV
10.95kX
5 μm

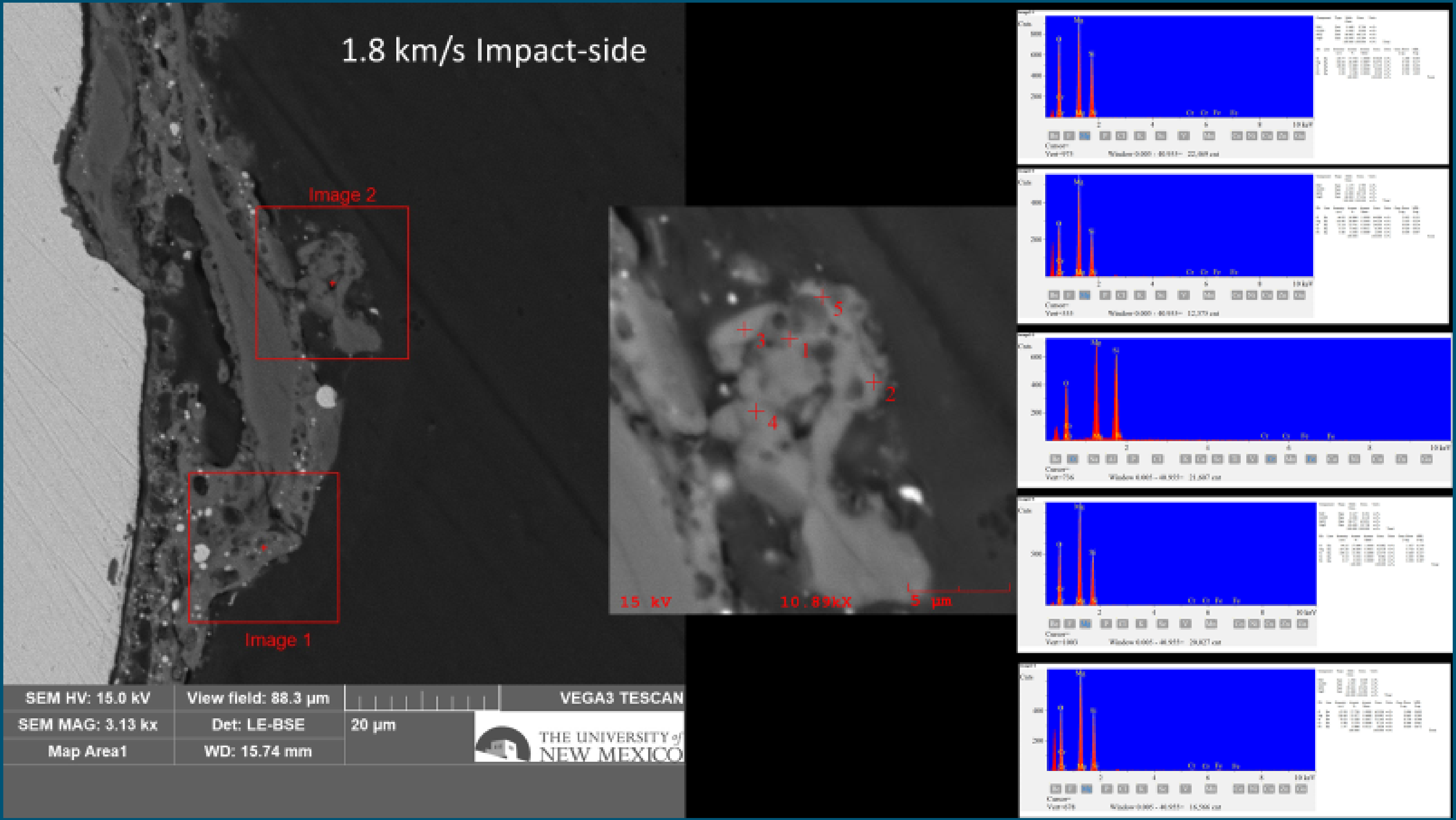

1.8 km/s Impact-side
Image 2
Image 1
SEM HV: 15.0 kV
View field: 88.3 μm
VEGA3 TESCAN
SEM MAG: 3.13 kx
Det: LE-BSE
20 μm
Map Area1
WD: 15.74 mm
THE UNIVERSITY of NEW MEXICO
5
3
1
2
4
15 kV
10.89kX
5 μm

Outline

- 1. Background:
  Study of high-pressure phases of olivine in meteorites
- 2. Methods:
  Experimental details and process
- 3. Results:
  From initial shock experiment campaign
- 4. Path forward

Path Forward

- 1. Make modifications to avoid loss of sample due to assembly separation
- 2. Execute shot campaigns with 20-60% iron content
- 3. Comparison of observed shock features with those found within shocked meteorites
- 4. Series of non-recovery shots to directly measure temperatures reached at fused silica/(ferro)periclase interface
- 5. Continued ALEGRA modeling refinement to constrain pressure and temperature conditions

Acknowledgements

- Sandia team: Marcus Knudson, Kyle Cochran, Kyle Cochran, and Shock Thermodynamic Applied Research Facilities (STAR) team – Shock experiments/design and hydrocode modeling
- Adrian Brearley – Focused ion beam (FIB) and Transmission electron microscope (TEM)
- Mike Spilde – Scanning electron microscope (SEM) and Electron microprobe (EMP)
- Jin Zhang – UNM high-pressure lab
- Chris Anderson – Design and modifications to a myriad of different hardware
- Carl Agee - Advisor
- Paul D. Asimow and Hannah Bausch – For sharing their insight and experience

(NASA/JPL-CALTECH)